Structural and Optical Properties of ZnO and Co Doped ZnO Thin Films Prepared by Sol-Gel

A.R. Khantoul[a], M. Sebais[a], B. Rahal[b], B. Boudine[a,*] and O. Halimi[a]

[a]Crystallography Laboratory, Physics Department, Faculty of Exact Sciences, Mentouri Brothers University, Route Ain El Bey, Constantine 25000, Algeria

[b]Spectrometry Department, Nuclear Technical Division, Nuclear Research Center of Algiers, 2 Bd., Frantz Fanon, BP 399, Algiers 16000, Algeria.

(Received October 5, 2017; in final form December 10, 2017)

We report on ZnO films doped with different Co concentrations (0, 0.5, and 1 wt%) prepared by sol-gel technique in association with dip-coating onto glass substrates. Zinc acetate dehydrate, cobalt acetate, mono ethanolamine were used as starting materials, as well as solvent and stabilizer, respectively. Nanostructured polycrystalline ZnO thin films with different concentrations of Co doping (0, 0.5, and 1 wt%) are prepared for the first time by the sol-gel method and annealed at 500 °C for 1 h. The surface morphologies of the ZnO thin films deposited on glass substrate with different concentrations were evaluated by atomic force microscopy. The optical absorption of the films showed a blue shift of the band gap. The photoluminescence signal of the thin films of undoped and Co-doped ZnO presents different bands in the visible region. The electrical conductivity of the sample with 0.5%Co was found to be 4.62 $(\Omega\ \mathrm{C\ m})^{-1}$.

DOI: 10.12693/APhysPolA.133.114

PACS/topics: Co doped ZnO, XRD, nanometric size, photoluminescence

1. Introduction

Zinc oxide (ZnO) is one of the most important oxide transparent conductors (TCO) materials attractive for applications. Usually ZnO adopts a hexagonal (wurtzite) crystal structure and presents n-type conductivity due to residual donors [1–4]. It is an interesting material for short-wavelength optoelectronic applications owing to its wide band gap 3.37 eV [5–7], large bond strength, large exciton binding energy (60 MeV) at room temperature, non toxic and abundant in nature [8–13]. Several techniques have been used for the preparation of ZnO thin films, such as sputtering, chemical vapor deposition (MOCVD), pulsed laser ablation (PLD), molecular beam epitaxy (MBE), electrochemical deposition, pyrolysis spray, reactive evaporation, colloidal and sol-gel method [14–19]. It is a versatile material that finds applications in various products, such as gas sensor, chemical sensor, biosensor, optical and electrical devices, window materials for displays, the thermal barrier, piezoelectric transducers, solar cells, varistors, laser devices and drug delivery [20–22].

In this work, undoped and Co doped ZnO thin films were prepared by the sol-gel method and deposited on glass substrates by dip-coating technique. The structural and optical properties of the obtained thin films were investigated.

2. Experimental

To obtain the undoped ZnO thin films, a solution of 0.17 mol/l was prepared by dissolving zinc acetate dehydrate ($Zn(CH_3CO_2{\cdot}2H_2O)$ in 2-methoxyethanol. After magnetic stirring for a few minutes at room temperature, the solution became white. The dropwise addition of monoethanolamine (MEA), with a molar ratio n MEA/$n$acetate = 1, rises the solubility of zinc acetate in the solvent and leads to a clear solution. The obtained solution is then heated under magnetic stirring at 60 °C for 2 h. The final solution is transparent and homogeneous. After that, it was left to stand in the fresh air for 24 h. The doping solution was then deposited on glass substrates by dip-coating technique. The prepared thin films were characterized by X-ray diffractometry (XRD) of type Pan Analytical using a Cu K_α radiation source (wavelength 1.5406 Å). Atomic force microscopy (AFM) (Nanocompact) operating in contact mode was employed for the observation of surface morphology for ZnO films with different concentrations of Co doping deposited on glass substrates. The optical properties of the ZnO thin films were determined by a UV-Vis spectrometer Shimadzu (UV-3101 PC) in the wavelength range 300–500 nm. The PL spectra measurements were carried out using a 250 nm lamp excitation from a Perkin-Elmer LS 50B luminescence spectrophotometer.

3. Results and discussion

3.1. X-ray diffraction analysis

Figure 1 shows the X-ray diffraction diagrams of undoped ZnO and Co doped ZnO films (0.5 wt% and 1 wt% Co) for all films that correspond to the hexagonal wurtzite structure of ZnO [23, 24]. The relative intensity of these peaks (002) orientation is predominant (0.5 wt% and 1 wt%Co). In principle the line (002) of 0.5 wt% is more intense than 1 wt%Co. It is noted that the intensity of the peaks decreases gradually with the increase

*corresponding author; e-mail: b_boudine@yahoo.fr

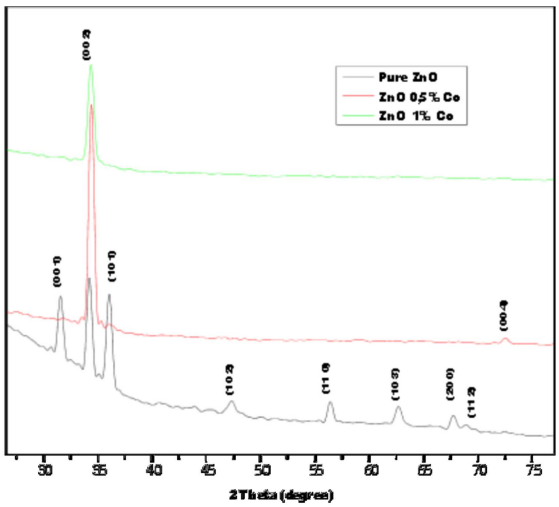

Fig. 1. Spectra of X-ray diffraction of ZnO thin films: undoped ZnO, ZnO doped 0.5 wt% Co and ZnO doped 1 wt% Co.

in cobalt content, which is due to the degradation of the crystal quality by the substitution of the Zn^{2+} ions by the Co^{2+} ions [24].

Crystallite sizes were determined based on (002) plane from XRD data of the samples.

In this experiment, the full width at half maximum (FWHM) was used with the Debye–Scherrer according to the formula [25, 26]:

$$D = \frac{0.9\lambda}{\beta \cos\theta}, \tag{1}$$

where D stands for the crystallite size in nm, λ refers to the wavelength value of the Cu K_α line ($\lambda = 1.5406$ Å), θ is the Bragg diffraction angle, β is the FWHM of the diffraction peak measured in rad.

The estimated crystallite size values are reported in Table I. This table demonstrates that all samples are nanometric grain size. An increase in Co concentration, decreases the grain sizes and grain boundaries increase.

TABLE I

Values of the grain size of undoped ZnO and n wt% Co doped ZnO thin films.

n	2θ [°]	FWMH [°]	(hkl)	D [nm]
0%	31.56	0.5793	(100)	14.25
	34.22	0.5723	(002)	14.52
	36.04	0.6333	(101)	13.20
	47.29	0.7823	(102)	11.09
	56.43	0.5847	(110)	15.43
	62.71	0.7038	(103)	13.22
	67.78	0.6270	(200)	15.27
	68.90	0.8381	(112)	11.50
0.5 wt%	34.41	0.5609	(002)	14.34
	72.56	0.6547	(004)	15.06
1 wt%	34.36	0.6222	(002)	13.37

3.2. Morphological characterization

Figure 2 represents the AFM images of the ZnO thin films deposited on glass substrates. From these images, we notice that the roughness mean square (RMS) value can be extracted and seems to be significantly dependent on the quantity of Co. An undoped sample presents an RMS of 6.7 nm; this value decreases from 28.1 to 14.7 nm for the 0.5 and 1 wt% of Co samples, respectively.

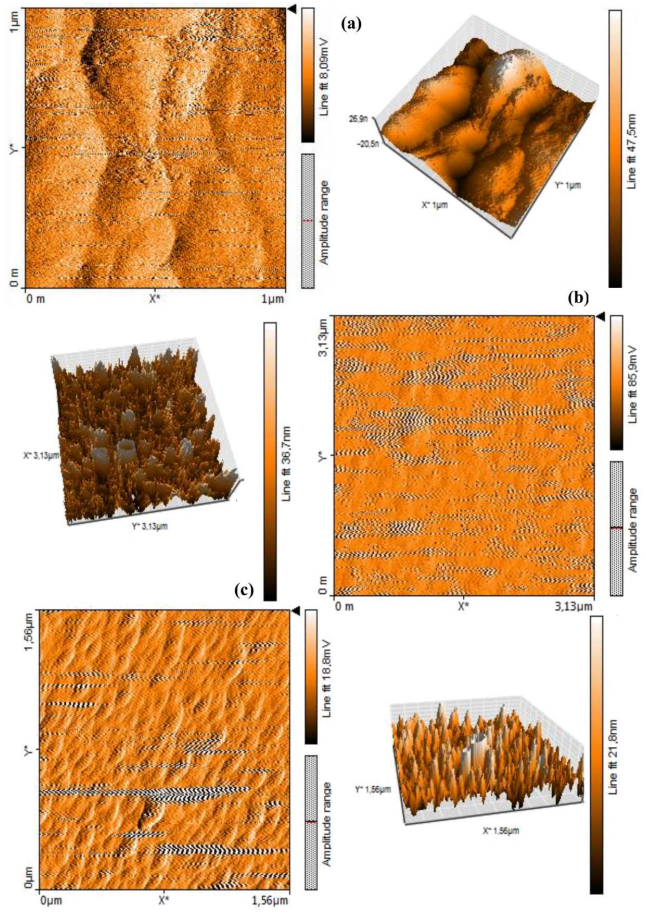

Fig. 2. AFM images of ZnO thin films deposited on glass substrates: (a) ZnO pure, (b) 0.5 wt% Co, and (c) 1 wt% Co.

3.3. Optical characterization

Figure 3 shows the optical transmittance spectra of Co doped ZnO thin films with different Co concentrations 0, 0.5, and 1 wt%. We observed that the transmittance of all the samples is close to 90%. We noticed also two distinct field of transmission wavelength:

- A domain identified by high absorption and low transmittance of light radiation to lower than 375 nm. We also note that the 1% Co doped substrate has the highest transmittance as 0.5% Co doped substrate is lower than 1% Co doped whereas undoped has the lowest value of transmission;

- An area of high transparency for the values that range between 375 and 500 nm (visible light). The transmittance in this field increases sharply and reaches between 90 and 100%.

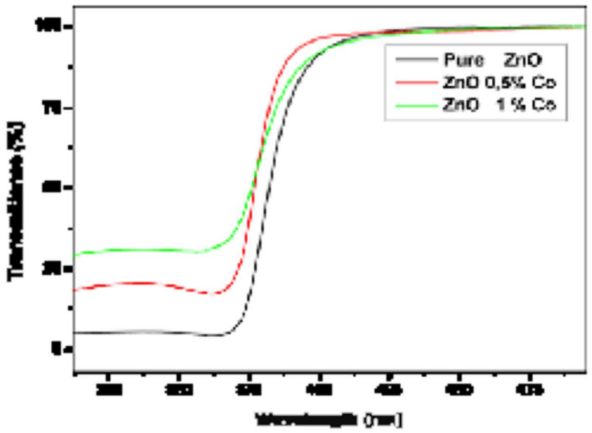

Fig. 3. Optical transmittance spectra of thin films: (a) undoped ZnO, (b) ZnO doped 0.5 wt% Co, and (c) ZnO doped 1 wt% Co.

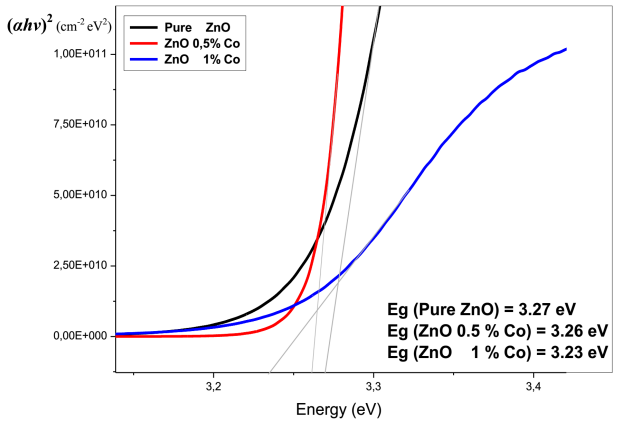

Fig. 4. Variation of the quantity $(\alpha h\nu)^2$ with energy for thin films (0, 0.5, and 1 wt% Co).

The band gap E_g was calculated using the Tauc equation [27]:

$$\alpha h\nu = A(h\nu - E_g)^n, \tag{2}$$

where $h\nu$ is the photons energy, E_g is the optical band gap energy, $n = 1/2$ for an indirect allowed transition and α is the absorption coefficient, which may be calculated from the transmittance using equation [28]:

$$\alpha = -\frac{1}{d \ln T}, \tag{3}$$

where d is the thickness of the film, T is the transmittance of the film.

Band gap energy, determined by the optical method, is obtained by extrapolating the linear portion of this graph to $(\alpha h\nu)^2 = 0$. As can be seen from Fig. 4, E_g (pure ZnO) is equal to 3.27 eV, E_g (0.5%) is equal to 3.26 eV and E_g (1%) is equal to 3.23 eV. The technique of band gap calculation is precise at a level of 0.01 eV.

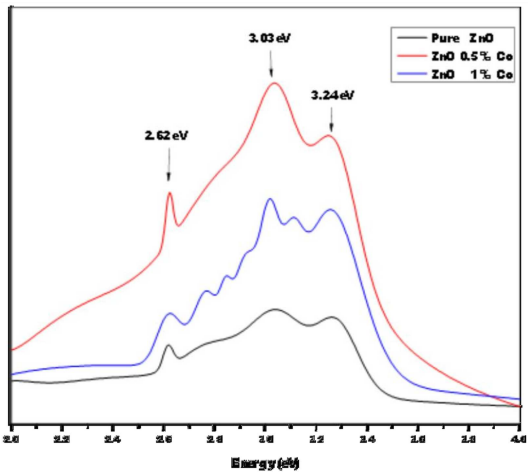

Fig. 5. PL spectra of undoped ZnO, ZnO doped 0.5 wt% Co and ZnO 1 wt% Co thin films.

It is noted that the band gap energy decreases from 3.27 to 3.23 eV with increasing cobalt concentration.

The photoluminescence of the Co doped ZnO films (Fig. 5) display a luminescence in the near UV in addition to the presence of three peaks. From Fig. 5, one can notice that the two peaks located at 2.62 eV and almost 3.01 eV are related to defects (zinc or oxygen interstitial position, oxygen vacancies etc.). The peak at 3.24 eV was attributed to the dopant [29].

3.4. Electrical properties

We have measured the conductivity of the films as a function of the cobalt concentration. Figure 6 shows the variation of the electrical conductivity of the undoped ZnO and the films doped with Co as a function of the doping Co. It is noted that the conductivity of the samples has decreased with the increase in doping (between 0% and 0.5% Co), has reached the minimum value up to 4.62 $(\Omega\ \mathrm{C\ m})^{-1}$, then increases to reach its maximum value of 5.90 $(\Omega\ \mathrm{C\ m})^{-1}$ at a concentration of 1% Co. This increase in conductivity with the increase in the Co concentration is attributed to an increase in the number of charge carriers (electrons).

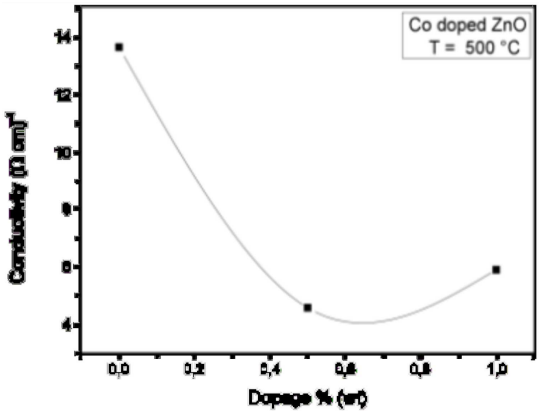

Fig. 6. Electrical conductivity of ZnO:Co as a function of the concentration of the dopant (Co).

4. Conclusions

In this work, we prepared the pure ZnO and Co-doped ZnO thin films on glass substrates by a sol–gel with dip-coating method. The ZnO thin films with different Co concentrations (0, 0.5, and 1 wt%) are polycrystalline with a texture along the *c*-axis [002]. The hexagonal wurtzite structure of ZnO does not change when Co^{2+} replaces Zn^{2+}. The grain sizes of the films are nanometric. The structural study indicates that 0.5 wt% Co-doping greatly improved the crystallization. When the doping concentration was increased, the crystallization quality dropped and grain size decreased. The optical measurement results confirm that all the ZnO thin films had high transmittance in the visible region 0.5 wt%. Co-doped ZnO thin film had the highest transmittance and the strongest ultraviolet emission. The optical gap of our ZnO samples decreases with the increase in Co concentration.

References

[1] D.C. Look, *Mater. Sci. Eng. B* **80**, 383 (2001).

[2] K. Ellmer, A. Klein, in: *Transparent Conductive Zinc Oxide — Basics and Applications in Thin Film Solar Cells*, Springer Series in Materials Science, Vol. 104, Springer-Verlag, Berlin 2008, p. 1.

[3] J.L. Chen, D. Chen, Z.H. Chen, *Sci. China Ser. E Tech. Sci.* **52**, 88 (2009).

[4] Z.L. Wang, *J. Phys. Condens. Matter* **16**, R829 (2004).

[5] K. Nakahara, H. Takasu, P. Fons, A. Yamada, K. Iwata, K. Matsubara, R. Hunger, S. Niki, *Appl. Phys. Lett.* **79**, 4139 (2001).

[6] C. Gumus, O.M. Ozkendir, H. Kavak, Y.J. Ufuktepe, *Optoelectron. Adv. Mater.* **8**, 299 (2006).

[7] M. Huang, S. Mao, H. Feick, H. Yan, Y. Wu, H. Kind, E. Weber, R. Russo, P. Yang, *Science* **292**, 1897 (2001).

[8] J. Song, S.A. Kulinich, J. Yan, Z. Li, J. He, C. Kan, H. Zeng, *Adv. Mater.* **25**, 5750 (2013).

[9] L. Ma, X. Ai, X. Huang, S. Ma, *Superlatt. Microstruct.* **50**, 703 (2011).

[10] C. Pan, L. Dong, G. Zhu, S. Niu, R. Yu, Q. Yang, Y. Liu, Z.L. Wang, *Nat. Photon* **7**, 752 (2013).

[11] C. Bundesmann, R. Schmidt-Grund, M. Schubert, in: *Transparent Conductive Zinc Oxide, Basics and Applications in Thin Film Solar Cells*, Eds. K. Ellmer, A. Klein, B. Rech, Springer Series in Materials Science, Vol. 104, Springer-Verlag, Berlin 2008, p. 79.

[12] E.K. Ellmer, A. Klein, B. Rech, *Transparent Conductive Zinc Oxide*, Eds. K. Ellmer, A. Klein, B. Rech, Springer Series in Materials Science, Vol. 104, Springer-Verlag, Berlin 2008.

[13] P.A. Rodnyš, I.V. Khodyuk, E.I. Gorokhova, S.B. Mikhrin, P. Dorenbos, *Opt. Spectr.* **105**, 908 (2008).

[14] S.W. Kim, S. Fujita, H.K. Park, B. Yang, H.K. Kim, D.H. Yoon, *J. Cryst. Growth* **292**, 306 (2006).

[15] J. Hu, R. Gordon, *Sol. Cells* **30**, 437 (1991).

[16] R.E. Marotti, D.N. Guerra, C. Bello, G. Machado, E.A. Dalchiele, *Sol. Energy Mater. Sol. Cells* **82**, 85 (2004).

[17] J. Zhao, L.Z. Hu, Z.Y. Wang, Y. Zhao, X.P. Liang, *Appl. Surf. Sci.* **22**, 311 (2004).

[18] K. Vinod, R.G. Singh, L.P. Purohit, R.M. Mehra, *J. Mater. Sci. Technol.* **27**, 481 (2011).

[19] R. Jayakrishnan, R. Sreekumar, K. Mohanachandran, C. Sudha Kartha, K.P. Vijayakumar, *Mater. Sci. Semicond. Process.* **16**, 326 (2013).

[20] Qing Hua Li, Deliang Zhu, Wenjun Liu, Yi, Lin, Xiao Cui Ma, *Appl. Surf. Sci.* **254**, 2922 (2008).

[21] M.H. Huang, S. Mao, H. Feick, H. Yan, Y. Wu, H. Kind, E. Weber, R. Russo, P. Yang, *Science* **292**, 1897 (2001).

[22] A. Raidou, M. Aggour, A. Qachaou, L. Laanab, M. Fahoume, *J. Condens. Mater.* **12**, 125 (2010).

[23] V. Shelke, B.K. Sonawane, M.P. Bhole, D.S. Patil, *J. Mater. Sci.* **23**, 451 (2012).

[24] Y. Caglar, *J. Alloys Comp.* **560**, 181 (2013).

[25] B.E. Warren, *X-Ray Diffraction*, Dover, New York 1990, p. 1.

[26] S. Karuppuchamy, J.-M. Jeong, D.P. Amalnerkar, H. Minoura, *Vacuum* **80**, 494 (2006).

[27] V. Jokanovic, A.M. Spasic, D. Uskokovic, *J. Coll. Interface Sci.* **278**, 342 (2004).

[28] D.M. Carballeda-Galicia, R. Castanedo-Pérez, O. Jiménez-Sandoval, S. Jiménez-Sandoval, G. Tores-Dalgado, C.L. Zũñiga-Romero, *Thin Solid Films* **371**, 105 (2000).

[29] L. Schmidt-Mende, J.L. MacManus-Driscoll, *Materials Today* **10**, 40 (2007).